Proceedings of the 11th International Conference on
Non-conventional Materials and Technologies (NOCMAT 2009)
6-9 September 2009, Bath, UK

ESTIMATION OF THE MECHANICAL PROPERTIES OF MUD SHEAR WALLS SUBJECTING TO LATERAL SHEAR FORCE

Kohei Komatsu[1], Akihisa Kitamori[2], Kiho Jung[3] and Takuro Mori[4]

[1,2,3,4] Research Institute for Sustainable Humanosphere, Kyoto University, Uji, Kyoto, Japan

Abstract: In this study, load-deformation relationship of mud shear wall (MSW) was assumed as a combined one which composed of non-linear semi-rigid frame action and non-linear solid wall action. In order to establish mechanical models, at first moment-rotation relationship of "Nuki" joint and mortise-tenon joint were theoretically derived. Then stress-strain relationship of solid mud part with bamboo laths was estimated by truncating load-deformation curve of frame only from that of full MSW. Finally, every data were inputted into non-linear FEM program to analyze three different MSW specimens. In the case of normal MSW, effect of frame was small, while in the case of hanging wall type MSW, the effect of frame joints was remarkable, especially in post yielding range.

Keywords: *Mud shear wall, "Nuki" joint, Mortise and Tenon joint, FEM analyses*

1. Introduction

Mud-shear wall (denoted as MSW) is one of the oldest types of shear walls for timber structures in Japan. So far as we know, the technique for making this kind of component as the walls of timber constructions was likely to be brought at the same time when Buddhism had been carried from the Continent to Japan in 6th to 7th century. Although MSWs have been used in Japan for more than 1400 years mainly in such large scale timber structures as temples, castles, relatively large scale residences and so on, it is said that its application and popularization to general people's town houses were in Edo-era, i.e., 17th century, mainly from the reason on the fire endurance requirement for wooden town houses.

Until recently almost no researchers except particular pure "timber research groups" have been paid any attentions on the mechanical properties of MSW, probably because it had been considered as an old fashion shear-resisting component which required not only long periods until completion but also special techniques for on site jobs, and more worth, the strength property of MSW was not sufficient as shear wall compared with newly coming such shear walls as nail-on plywood shear wall.

Being affected, however, by so-called "conscious on environmental problems", many researchers (for example, Nakao et al. 2005) have begun to pay new attention on MSWs once again recently due to the reasons why they can be composed of such sustainable and

[1]Professor, *kkomatsu@rish.kyoto-u.ac.jp*
[2]Assistant Professor, *kitamori@rish.kyoto-u.ac.jp*
[3]Mission Research Scientist, *jungkiho@rish.kyoto-u.ac.jp*
[4] Assistant Professor, *moritakuro@rish.kyoto-u.ac.jp*

environmentally-friendly natural materials as timber, bamboo, rice straw and mud.

In this paper, we would like to propose a practical engineering method for predicting nonlinear behaviours of MSWs by employing nonlinear FEM program in conjunction with recent theoretical development on wooden 'Nuki' joint and previous experimental studies on full scale MSWs

2. Experimental

We had carried out a series of lateral loading tests on three deferent kinds of shear wall specimens in 2004 (Tabuchi et al. 2006), therefore in this paper the experimental results will be quoted for verification of numerical analysis. Figures 1, 2 and 3 show configuration and real features of three different MSW specimens employed. Table 1 shows common specification in MSW and some physical properties of timbers.

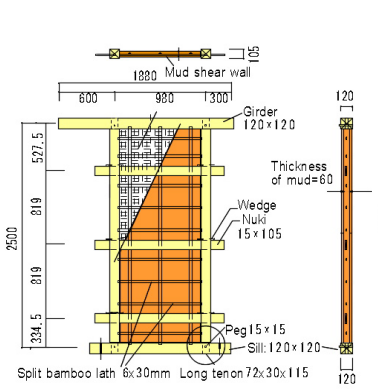

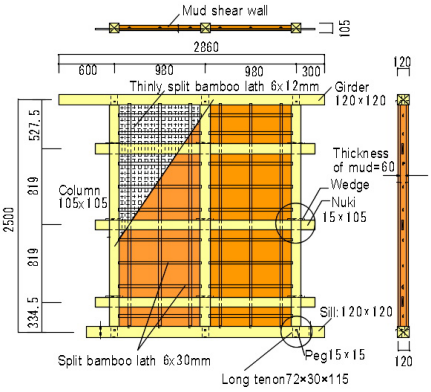

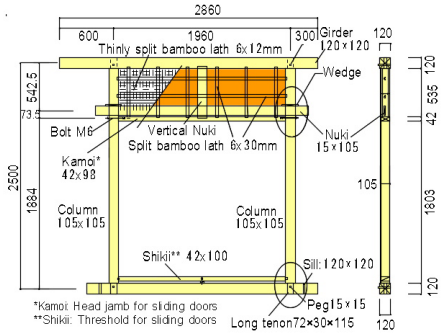

Figure1: 1P-MSW

Figure2: 2P-MSW

Figure3: 2P-Hanging wall

Table1: Common specification in MSW and some physical properties of timbers used

Part (in mm)	***Species***	***Cross section* (mm)**	***Remarks***
Peg	Oak	15 x 15	
Wedge	Japanese Cedar	*h* (16-9) x *L*91 x *t*14	from both sides
Bamboo lath	Madake	large :*w* (24-30) x *t* (3-9)	fine: *w* (12-18) x *t* (3-9)
Course mud : *t* (42)	Course mud with rice straw *t* (30) + fine mud *t* (6) on both surface		
Fine mud : *t* (18)	Fine mesh mud with sand and rice straw *t* (18)		
Column (105 x 105)	Japanese Cedar	MOE=8660 N/mm^2	Density=375 kg/m^3
Sill (120 x 120)	Japanese Cedar	MOE=11220 N/mm^2	Density=375 kg/m^3
Girder (120 x 120)	Japanese Cypress	MOE=10790 N/mm^2	Density=420 kg/m^3
Nuki (15 x 105)	Japanese Cedar	*MOE=8660 N/mm^2	Density=375 kg/m^3

*Dynamic MOE of Nuki measured on site was very low thus assumed as the same as column.

Static push-pull cyclic lateral load was applied using 294kN capacity oil jack by controlling jack movement in accordance with a loading protocol as shown in Figure 4.

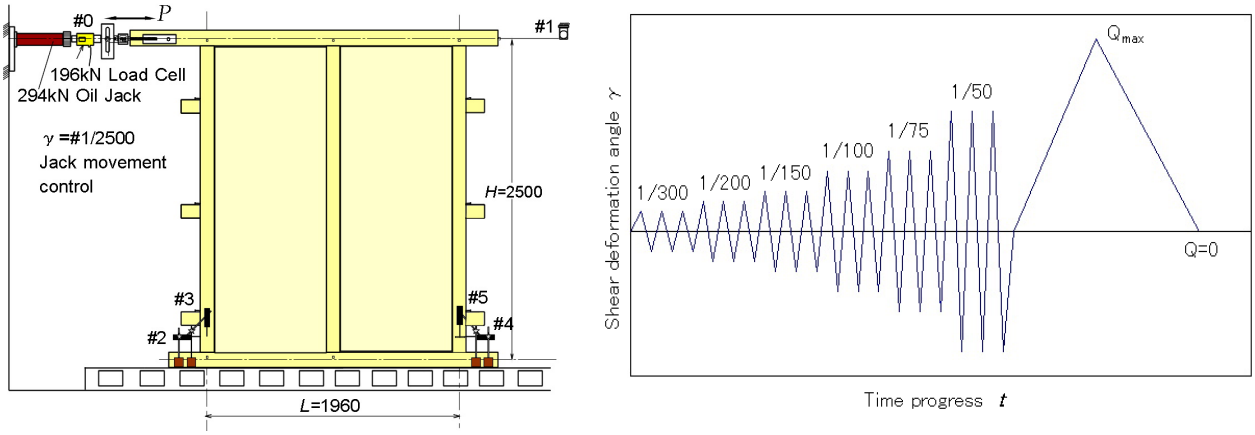

Figure 4: Test set-up and **l**oading protocol.

3. Theory

3.1 Moment-Rotation Angle Relationship of Frame Joint

In order to take the effects of frame's performance into analysis, we derived non-linear moment-rotational angle relationships of column-sill joint or column-girder joint as well as column-"Nuki" joint on the basis of Kitamori's modified analytical model (Kitamori 2009, Kitamori et. al 2009a, Kitamori et al 2009b).

["Nuki" joint (Column-thin beam pass through joint)]

Figure 5 indicates schematic diagram of assumed deformation in the Nuki joint in which reaction forces, N due to embedment on Nuki and C due to "additional length effect" on Nuki in conjunction with friction effect, generate a resisting moment M_{by} around at the centre of Nuki joint as shown in equation (1) before yielding angle θ_y.

$$M_{by} = \left\{ \left(\frac{2X_p}{3} + \mu Z_0 \right) N_e + \left(X_p + \mu Z_0 \right) C_e \right\} \theta \qquad (0 \le \theta \le \theta_y) \qquad \ldots(1)$$

where,

$$N_e = \frac{X_p^{\,2} Y_p E_\perp}{8 Z_0} \qquad \ldots(2) \qquad C_e = \frac{X_p Y_p E_\perp}{2 a Z_0} \qquad \ldots(3) \qquad a = \frac{5.5}{Z_0} \qquad \ldots(4)$$

While in the range of post yielding angle θ_y, contribution from embedment was assumed to be saturated thus resisting moment M_{py} could be approximately derived in a 'closed non-linear form' by Kitamori(2009) as shown in equation (5).

$$M_{py} = \left\{ \left(\frac{2X_p}{3} + \mu Z_0 \right) \left(2 - \frac{\theta_y}{\theta} \right) N_e + \left(X_p + \mu Z_0 \right) \left(1 - \log_e \frac{\theta_y}{\theta} \right) C_e \right\} \theta_y \qquad (\theta \ge \theta_y) \ldots(5)$$

where,

$$\theta_y = \frac{Z_0 F_m}{X_p E_\perp \left(1 + \frac{2Z_0}{aX_p}\right)} \qquad \ldots(6)$$

here,

$E_\perp$: Modulus of elasticity of Nuki material perpendicular to the grain (=$E_\parallel$/25)

F_m : Basic embedment strength of Nuki material

θ : Rotational angle at Nuki joint

X_p, Y_p, Z_0 : Size of Nuki joint shown in Figure 5-(a)

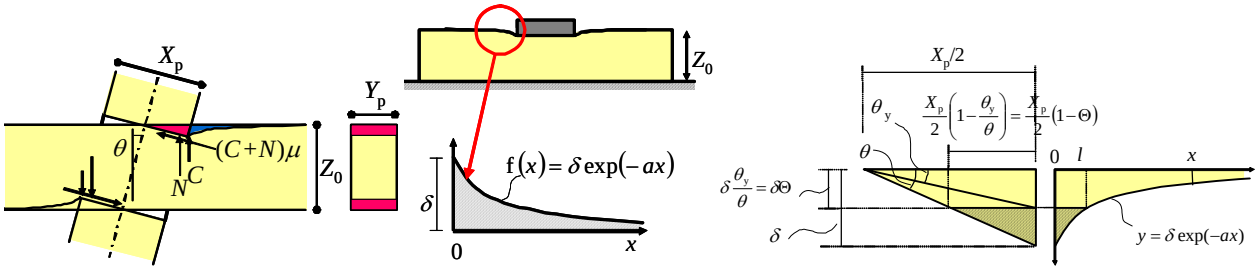

(a) Equilibrium of forces (b) Additional length effect (c) Post yielding assumption

Figure 5: Schematic diagram of assumed deformation and forces in Nuki joint

[Mortise and Tenon Joint (Girder-Column or/and Sill-Column Joint)]

a) Nuki Effect in Mortise and Tenon Joint

Figure 6 shows schematic diagram of Nuki effect in mortise and tenon joint in which reaction forces, N_1, N_2 due to embedment of tenon and C_1 due to "additional length effect" of tenon in conjunction with friction effect, generate a resisting moment M_{by} at around *rotation* centre of mortise and tenon joint as shown in equation (7) before yielding angle θ_y.

$$M_{by} = \left\{\frac{2e}{3}N_{1e} + \left(X_p - e + \mu Z_0\right)N_{2e} + eC_{1e}\right\}\theta$$

$$(0 \le \theta \le \theta_y) \qquad \ldots(7)$$

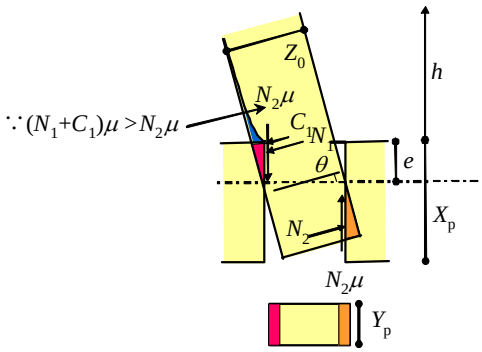

Figure 6: Schematic diagram of "Nuki" effect in mortise and tenon joint

where,

$$N_{1e} = \frac{e^2 Y_p E_\perp}{2Z_0} \ldots(8) \qquad N_{2e} = \frac{\left(X_p - e\right)^2 Y_p E_\perp}{2Z_0} \qquad \ldots(9) \qquad C_{1e} = \frac{X_p Y_p E_\perp}{2aZ_0} \ldots(10)$$

$$e = \frac{2X_p^{\,3} + 3hX_p^{\,2}}{3X_p^{\,2} + 6hX_p + \frac{6h}{a}} \qquad \ldots(11) \qquad a = \frac{5.5}{Z_0} \quad \ldots \qquad (12)$$

While in the range of post yielding angle θ_y, resisting moment M was derived in accordance with the same assumption as was done in Nuki joint and its result is shown in equation (13).

$$M_{py} = \left[\left\{\frac{2e}{3}N_{1e} + \left(X_p - e + \mu Z_0\right)N_{2e}\left(2 - \frac{\theta_y}{\theta}\right) + eC_{1e}\left(1 - \log_e \frac{\theta_y}{\theta}\right)\right\}\right]\theta_y \qquad (\theta \geq \theta_y) \ldots(13)$$

where, θ_y is shown in equation (6) and another variables should be refereed in Figure 6.

b) Dowel Effect in Mortise and Tenon Joint

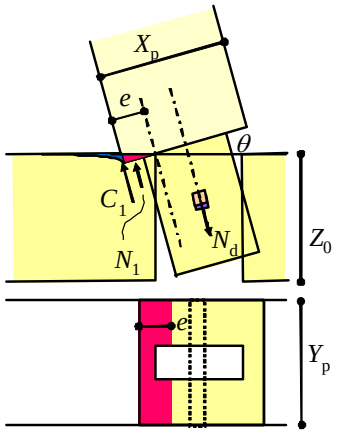

Figure 7: Schematic diagram of Dowel effect in mortise and tenon joint

Figure 7 shows schematic diagram of dowel effect in mortise and tenon joint in which reaction forces, N_1, due to embedment on sill, C_1 due to "additional length effect" on sill and dowel effect N_d due to shear resistance of peg in conjunction with friction effect, generate a resisting moment M_{by} at around *rotation* centre of mortise and tenon joint as shown in equation (14) before yielding angle θ_y.

$$M_{by} = \left\{\left(\frac{2}{3}N_{1e} + C_{1e}\right)e + \left(\frac{X_p}{2} - e\right)N_{de}\right\}\theta \qquad (0 \leq \theta \leq \theta_y) \ldots(14)$$

where,

$$e = \frac{-\left(Z_0 K_d + \frac{Y_p E_\perp}{a}\right) + \sqrt{\left(Z_0 K_d + \frac{Y_p E_\perp}{a}\right)^2 + Y_p X_p Z_0 K_d E_\perp}}{Y_p E_\perp} \quad \ldots(15)$$

$$N_{de} = \left(\frac{X_p}{2} - e\right)K_d \quad \ldots(16)$$

here, K_d is a pull-out stiffness of peg-tenon-sill three layers system. Other valuables are the same as those in the clause for Nuki effect.

While in the range of post yielding, we assumed that resisting moment remained constant, namely, perfect bi-linear assumption was employed. The criterion of yield was assumed when peg reached its yielding strength. Hence equation (17) was given for post yield moment M_{py}

$$M_{py} = \left\{\left(\frac{2}{3}N_{1e} + C_{1e}\right)e + \left(\frac{X_p}{2} - e\right)N_{de}\right\}\theta_y \qquad (\theta \geq \theta_y) \ldots(17)$$

where,

$$\theta_y = \frac{P_{dy}}{K_d}\left(\frac{2}{X_p - e}\right) \quad \ldots(18)$$

here, P_{dy} is a yielding shear strength of peg-tenon-sill joint.

Consequently, every $M - \theta$ relationship of frame joints were approximated by bi-linear relationship as shown in Figure 8, in which that of mortise and tenon joint became tri-linear by combined two bi-near lines.

Nuki Joint Rn		
γ (rad)	M (Nm)	Rn (Nm/rad)
0.0000	0.0	
0.0265	301.6	11368
0.1000	426.3	1697
Nuki Effect in Mortise and Tenon Joint		
γ (rad)	M (Nm)	$R_{mt\text{-}n}$ (Nm/rad)
0.0000	0.0	
0.0198	461.0	23302
0.1000	578.4	1464
Dowel Effect in Mortise and Tenon Joint		
γ (rad)	M (Nm)	$R_{mt\text{-}D}$ (Nm/rad)
0.00000	0.0	
0.04045	505.9	12507
0.10000	505.9	0
Combined Mortise and Tenon Joint Rh		
γ (rad)	M (Nm)	Rh (Nm/rad)
0.00000	0.0	
0.01978	708.4	35809
0.04045	997.2	13971
0.10000	1084.3	1464

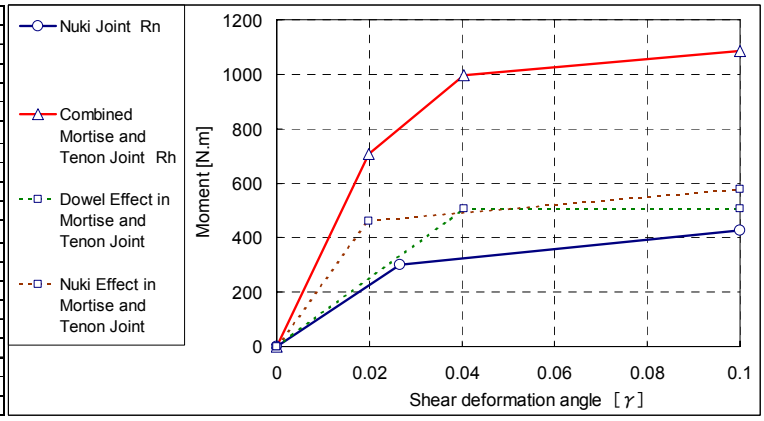

Figure 8: Approximated Poly-Linear $M-\theta$ Relationship of Frame Joints.

3.2 Assumptions on the Stress-Strain Relationship of Mud with Bamboo Laths

Shear stress-shear strain relationship (τ - γ) of mud wall with bamboo laths might be estimated by truncating load–shear strain relationship (Q_{Frame} - γ) of frame only from that ($Q_{MSW}-\gamma$) of perfect MSW and divided by cross section area ($A_{MSW}=t\cdot L$) of MSW, where t .is thickness and L is length of wall. Figure 9-a) shows this procedure in which from averaged $Q_{MSW}-\gamma$ data set of MSW obtained from experiments on 2P-MSW specimens, $Q_{Frame}-\gamma$ data set was truncated then (τ - γ) relationship was obtained by divided with wall cross section area.

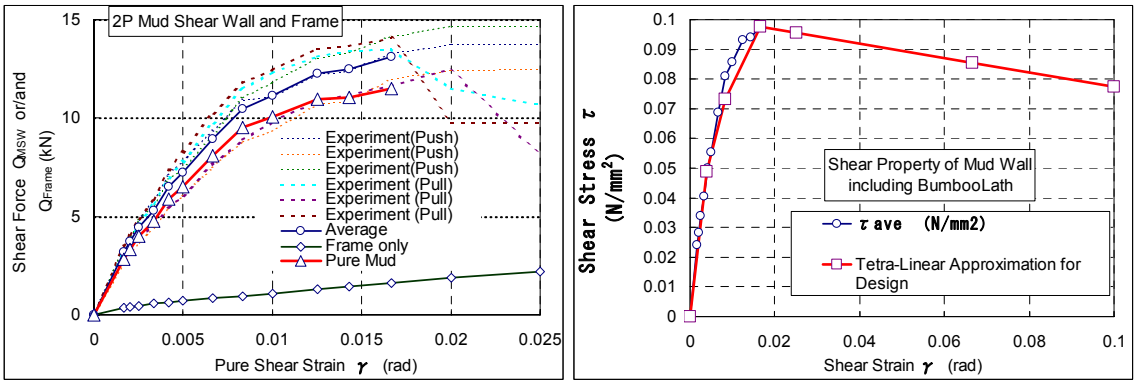

(a) ($Q_{MSW}-\gamma$) – ($Q_{Frame}-\gamma$)=($Q_{mud}-\gamma$) (b) (τ - γ) relationship of mud part

Figure 9: Procedure for getting (τ - γ) relationship of mud with bamboo laths.

Obtained (τ - γ) relationship was approximated by a tetra-linear relationship as shown in equation (19) for nonlinear FEM analysis in latter section as shown in Figure 9(b).

$$\tau\left(\gamma=\frac{1}{240}\right)=0.5\tau_0,\qquad \tau\left(\gamma=\frac{1}{120}\right)=0.75\tau_0,\qquad \tau\left(\gamma=\frac{1}{60}\right)=1.0\tau_0$$

$$\tau=\tau_0\left(\frac{25}{24}-\frac{60}{24}\gamma\right)\qquad \text{for}:\ \left(\frac{1}{60}\le\gamma\le\frac{1}{10}\right)\qquad\qquad \ldots(19)$$

here, τ_0 is the maximum shear stress that depends on characters of mud, bamboo lath and so on. In this study, this value was evaluated as 0.0977N/mm^2.

3.3 Replacement of Stress-Strain Relationship of Mud Part to Equivalent Spring of Brace

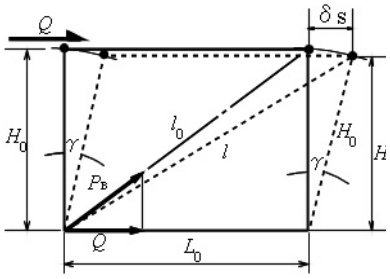

Figure 10:
Replacement of Mud Part to Equivalent Brace.

For calculating nonlinear behaviour of MSW until final stage using commercial FEM program, shear stress-strain tetra-linear relationship of mud part was replaced to a tetra-linear relationship of equivalent spring as follows; From geometrical relationship shown in Figure 10, elongation of equivalent spring δ_B can be expressed as equation (20).

$$\delta_B = l - l_0 = \sqrt{H^2 + \left(L_0{}^2 + \delta_s\right)^2} - \sqrt{H_0{}^2 + L_0{}^2} \quad \ldots(20)$$

While, lateral displacement of rectangular mud part δ_s has a relationship with shear strain γ as shown in equation (21).

$$\delta_s = \gamma \cdot H_0 \quad \ldots(21)$$

Combining equations (20), (21) and applying the binomial theorem, $|z| < 1, (1+z)^m \approx 1 + mz$, we got equation (22).

$$\delta_B \approx \frac{L_0}{l_0}\delta_s \quad \ldots(22)$$

While equation (23) is derived from shear stress-strain relationship of mud part with bamboo lathes.

$$\tau = G \cdot \gamma \rightarrow \frac{Q}{L_0 t} = G\frac{\delta_s}{H_0} \rightarrow Q = \frac{GL_0 t}{H_0}\delta_s \quad \ldots(23)$$

Relationship between Q and equivalent brace force P_B is given in equation (24).

$$Q = \frac{L_0}{\sqrt{L_0{}^2 + H_0{}^2}}P_B \quad \ldots(24)$$

Combining equations (22), (23) and (24), we got a force-elongation relationship of equivalent brace including various parameters of original mud part as in equation (25).

$$P_B = Gt\left(\frac{L_0}{H_0} + \frac{H_0}{L_0}\right)\delta_B \quad \ldots(25)$$

where,
G : Shear rigidity of mud part including bamboo laths (this value depends on γ range)
t : Thickness of MSW.
L_0 and H_0 : Dimensions of original rectangular mud part including bamboo lathes.

4. FEM Analyses

Figures 11-(a), (b) and (c) show FE-modelling of three different MSW specimens and comparisons between computed results with experimental envelope curves which indicate peak point data selected from the full data set of push-pull cyclic loading data. All computations were carried out using a commercial FEM software, developed for 3D-frame structures called as Snap-Ver.3 by Kozo System / Kentiku Pivot Co., Ltd., which runs on the plat home of Windows XP® system.

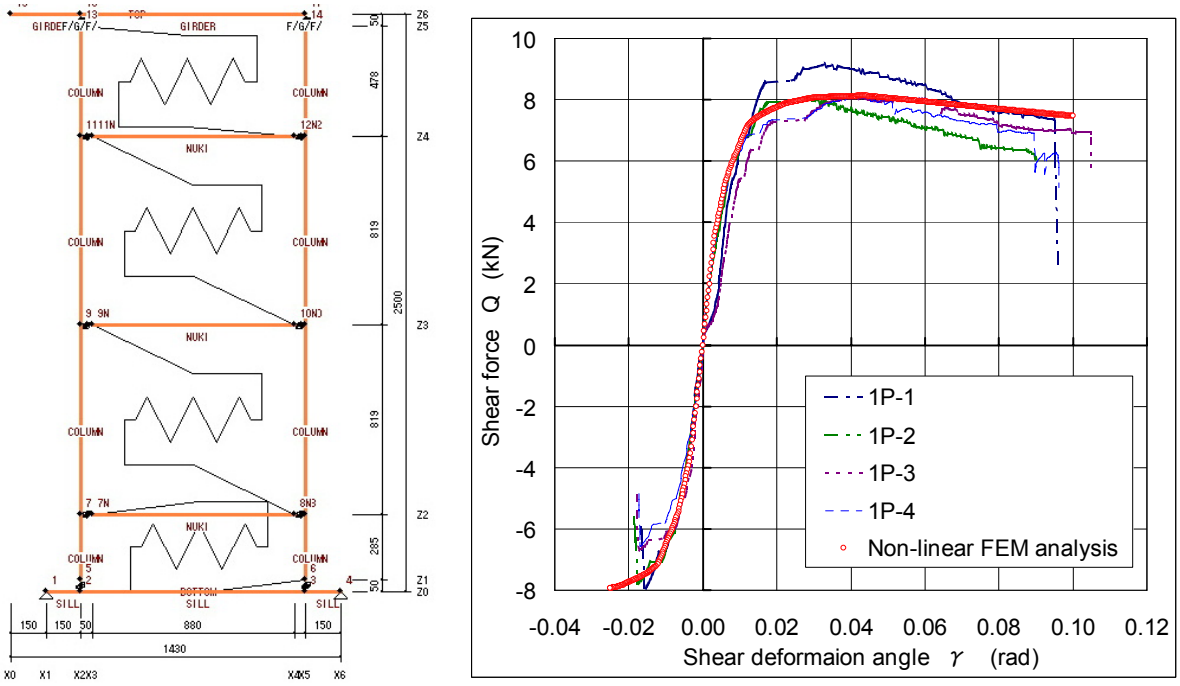

Figure 11-(a) FE-modelling and comparisons between a computed result and experimental results on1P-MSW specimen.

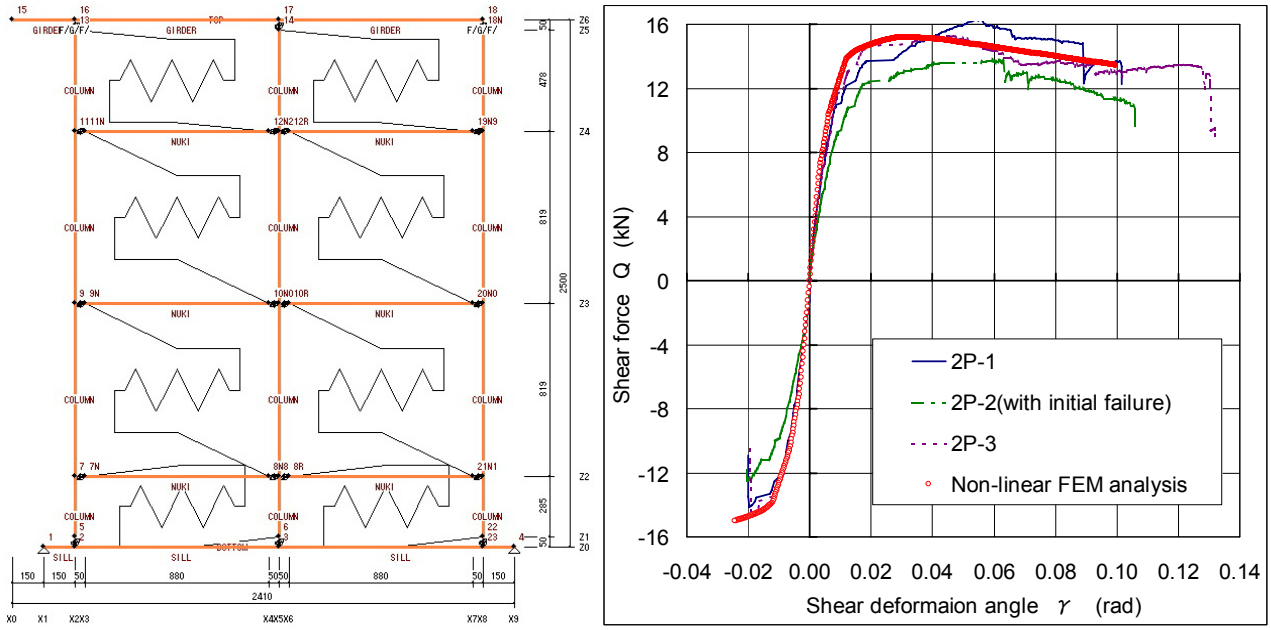

Figure 11- (b) FE-modelling and comparisons between a computed result and experimental results on 2P-MSW specimen.

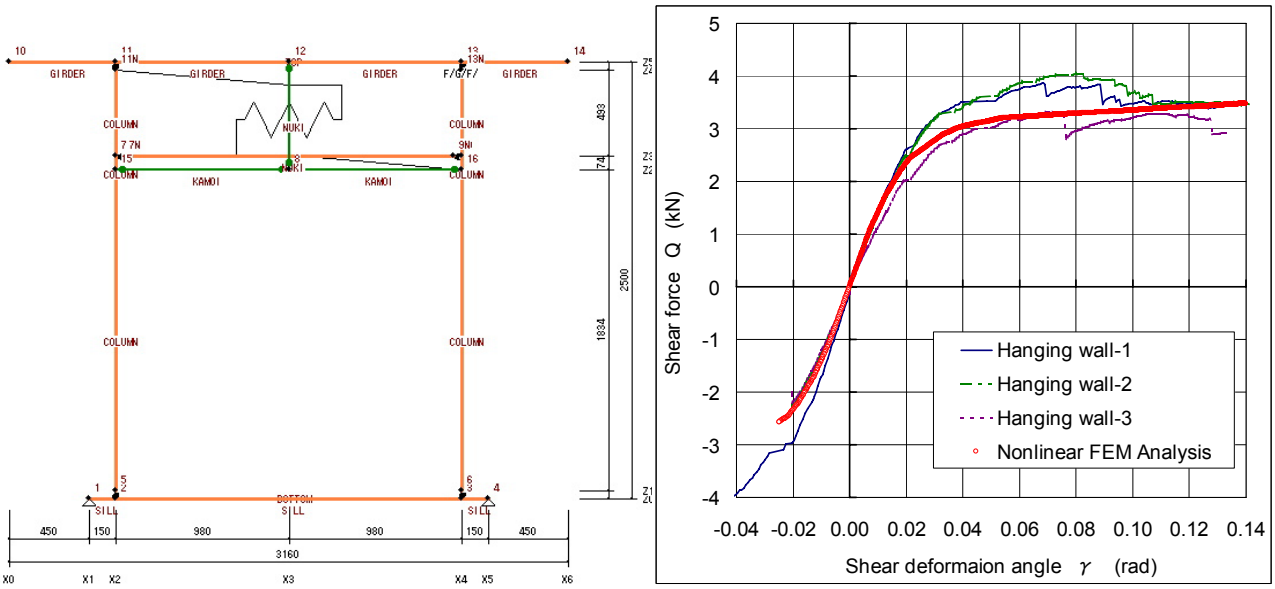

Figure 11- (c) FE-modelling and comparisons between a computed result and experimental results on 2P-Hanging wall specimen.

5. Results and Discussion

From comparisons between computed results with experimental envelope curves shown in Figures 11-(a), (b) and (c), it is obvious that mechanical models proposed in this study were likely to be appropriate. In the case of full wall specimens such as 1P or/and 2P specimens, contributions from frame joint resistances seemed to be relatively small because computed results clearly reflected decreasing stiffness characteristics of mud part. On the other hand, in the case of hanging wall type specimen shown in Figures 11-(c), contribution from frame joint resistances were remarkable especially in the post yielding range because computed result reflected increasing stiffness characteristic of Nuki or/and mortise and tenon joint after yielding range.

In this paper, the strength properties of MSW were obtained by truncating load–shear strain relationship (Q_{Frame}-γ) of frame only from that ($Q_{MSW}-\gamma$) of perfect 2P-MSW specimens, therefore it might be said as “matter of course” that FEM analysis agreed well with experimental data. We think, however, it is important that the FEM analyses could also precisely predict mechanical properties of another types of specimen such as 1P-MSW or/and hanging wall type specimens.

6. Conclusions

In this paper, three different types of mud shear walls were computed using commercial FEM program by assuming that most frame joints acted as non-linear semi-rigid joint as well as mud part including bamboo laths could be replaced by equivalent non-linear brace. Comparisons between computed results with experimental results were fairly good. From these results, it might be concluded that modelling methods taken in this study was thought to be appropriate.

7. Acknowledgements

Part of this study was supported by a budget given by the Japan Society for Promoting Science (JSPS). The authors would like to express their sincere appreciations for JSPS.

8. References

KITAMORI, A. 2009. *Evaluation and Improvement of Wooden "Kangou" Joints due to Embedment and Friction*, Ph.D Thesis submitted to Kyoto University. (in Japanese)

KITAMORI, A., MORI, T., KATAOKA, Y. and KOMATSU, K. 2009a. *Effect of Additional Length on Partial Compression Perpendicular to the Grain of Wood*, Journal of Structural and Construction Engineering. Transactions of Architectural Institute (AIJ) of Japan, in press (in Japanese)

KITAMORI, A., JUNG, K., MINAMI, M. and KOMATSU, K. 2009b. Evaluation on Stiffness of Lattice Shear Wall, Influence of gap and its verification by long term test, Journal of Structural Engineering, AIJ, Vol.55B, pp.109-116. (in Japanese)

NAKAO, M., ICHIMONJI, R., YAMAZAKI, Y. and ISHIBASHI, Y. 2005. *An Experimental Study on Shear Resisting Mechanism and Shear Strength Evaluation Method of Mud-Plaster Walls*, Journal of Structural and Construction Engineering. Transactions of AIJ, **598**, pp.109-116. (in Japanese)

TABUCHI, A., KITAMORI, A., MORI, T., and KOMATSU, K. 2006. *Lateral Shear Performance of Earth-Wall in Case of A Town House of Kyoto.* Journal of Structural and Construction Engineering. Transactions of AIJ, **598**, pp.109-116. (in Japanese)